

Optical properties of the iron-based superconductor LiFeAs single crystal

Byeong Hun Min¹, Jong Beom Hong², Jae Hyun Yun³, Takuya Iizuka⁴, Shin-ichi Kimura^{4,5}, Yunkyu Bang^{3,6,†}, Yong Seung Kwon^{1,§}

¹Department of Emerging Materials Science, Daegu Gyeongbuk Institute of Science and Technology (DGIST), Daegu 711-873, Republic of Korea

²Department of Physics, Sungkyunkwan University, Suwon 440-746, Republic of Korea

³Department of Physics, Chonnam National University, Kwangju 500-757, Republic of Korea

⁴School of Physical Sciences, The Graduate University for Advanced Studies, Okazaki 444-8585, Japan

⁵UVSOR Facility, Institute for Molecular Science, Okazaki 444-8585, Japan

⁶Asia Pacific Center for Theoretical Physics, Pohang 790-784, Republic of Korea

E-mail: †ykbang@chonnam.ac.kr

E-mail: §yskwon@dgist.ac.kr

Abstract. We have measured the reflectivity spectra of the LiFeAs ($T_c = 17.6$ K) single crystal in the temperature range from 4 to 300 K. In the superconducting (SC) state ($T < T_c$), the clean opening of the optical absorption gap was observed below 25 cm^{-1} , indicating an isotropic full gap formation. In the normal state ($T > T_c$), the optical conductivity spectra display a typical metallic behavior with the Drude type spectra at low frequencies, but we found that the introduction of the two Drude components best fits the data, indicating the multiband nature of this compound. A theoretical analysis of the low temperature data ($T = 4 \text{ K} < T_c$) also suggests that two SC gaps best fit the data and their values were estimated as $\Delta_1 = 3.3 \text{ meV}$ and $\Delta_2 = 1.59 \text{ meV}$, respectively. Using the Ferrell-Glover-Tinkham (FGT) sum rule and dielectric function $\epsilon_1(\omega)$, the plasma frequency of the SC condensate (ω_{ps}) is consistently estimated to be $6,665 \text{ cm}^{-1}$, implying that about 65 % of the free carriers of the normal state condenses into the SC condensate. To investigate the various interband transition processes (for $\omega > 200 \text{ cm}^{-1}$), we have also performed the local-density approximation (LDA) band calculation and calculated the optical spectra of the interband transitions. This theoretical result provided a qualitative agreement with the experimental data below 4000 cm^{-1} .

PACS numbers: 74.25.Gz, 74.20.Rp, 74.70.Xa

1. Introduction

Iron based superconductors, i.e. $\text{ReFeAsO}_{1-x}\text{F}_x$ (Re: rare-earth elements), AFe_2As_2 (A: alkali metal), FeSe , and AFeAs (A: alkali metal) [1, 2, 3, 4, 5, 6, 7, 8, 9], have become the focus of intensive research in the hope of understanding the pairing mechanisms of the unconventional superconductivity based on the $3d$ electrons. Among the iron based superconductors, LiFeAs is unique because of its simple crystalline structure and its moderately high superconducting (SC) transition temperature ($T_c \sim 17$ K) without doping. The theoretical band calculations have predicted a multiband nature (up to a maximum of five conduction bands) of this compound, which was confirmed experimentally [10, 11, 13]. Hence the various SC properties are expected to show the multi-bands and multi-gaps nature such as: specific heat measurements (C_p), tunnel diode resonator measurement (TDR), microwave surface impedance measurements, lower critical field studies (H_{c1}), Raman spectroscopy and angle resolved photoemission spectroscopy (ARPES) [13, 14, 15, 16, 17, 18, 19, 20]. However, in most of experimental measurements, except ARPES, the SC gaps were estimated indirectly, and therefore the estimated values should contain a degree of uncertainty. Even in the case of ARPES, although the SC gap sizes are directly measured, it probes only surface states and also has the problem of the surface degradation.

Far infrared spectroscopy is a powerful tool for investigating the bulk properties of the electronic structure of materials such as the changes of the Fermi surfaces (FSs) and low energy excitations, and hence it can directly measure the SC energy gap sizes of the bulk state. The studies of the SC gap by the far infrared spectroscopy have already been reported for 1111, 122, 11 and 245 systems [21, 22, 23, 24, 25, 26, 27, 28, 29, 30, 31] but until now it has not yet been reported for LiFeAs system. In the case of LiFeAs , especially, the accurate measurement of the spectrum below 100 cm^{-1} is very important for examining the SC gap(s) and the multiband nature because its T_c is relatively lower than other iron based superconductors studied with the optical spectroscopy.

In this study, we report the optical measurements of LiFeAs single crystal with $T_c = 17.6$ K. In particular, we have measured the reflectivity data down to 15 cm^{-1} in order to resolve the SC gap formation. To control the uncertainty level at far-infrared and tera-hertz frequency region, we have used our specially designed feedback positioning system [32]. Below T_c , we have observed the clear signatures of the SC gap formation in the reflectivity data which becomes flat and approaches unity at low frequencies. In the real part of the optical conductivity, which is obtained by the Kramers-Kronig (KK) relation from our reflectivity data, this feature is identified as the opening of the optical absorption gap at low frequencies. Theoretical fitting using the generalized Mattis-Bardeen formula [33] yields the best result with two SC gaps with the estimated sizes as 1.59 and 3.3meV, respectively. These two gap values are in perfect agreement with the estimate from the specific heat measurement [12]. Also the larger gap value is consistent with the already reported results [13, 14, 16, 18, 19, 17, 34] by other experimental probes. We also showed that the normal state optical conductivity can be best understood by

introducing two Drude spectral components, which consistently supports the multiband nature of LiFeAs superconductor.

2. Experimental details

The single crystal of LiFeAs was grown by a closed Bridgeman method [8] and the size of obtained single crystal is approximately 3 mm \times 3 mm with shiny surface. The single crystal has a layer structure with a cleaved surface perpendicular to c -axis, [001] direction. Performing the optical measurement on LiFeAs is a challenge due to its quick degradation in air [17]. In order to avoid the degradation of the sample, it was cleaved in a high purity Helium gas filled glove bag and the sample was attached to the optical sample holder under Helium gas atmosphere. Electrical resistivity measurement was carried out using the standard four probe method. Reflectivity measurements were carried out on the freshly cleaved single crystal surface (ab -plane). JASCO FTIR610 was used for the infrared reflectivity spectroscopy in the frequency range from 40 to 12,000 cm^{-1} for temperatures of 4 \sim 300 K. To improve accuracy in the frequency region below 100 cm^{-1} , JASCO FARIS was used for the THz frequency range from 15 to 200 cm^{-1} for the same temperatures. ACTON VM 504 spectrometer was used for visible and violet reflectivity spectroscopy in the frequency range from 9,000 to 40,000 cm^{-1} . An in-situ gold evaporation technique was used to calibrate for the absolute reflectivity value. Sample size of most of the iron based superconductors, including ours, is smaller than the beam size ($\phi \sim 8$ mm), so that the interference from the sample edge and the on-passing optical window occurs and becomes the main source of uncertainty. Thus we have specially designed the feedback positioning system to suppress this type of uncertainty [32, 35]. A small reference mirror, which will be used for locating the reference point, is attached on the opposite side of the sample holder and thus searches for the maximum intensity of the reflected laser with Si diode. The resolution of stepping motor being used for vertically shift is 0.1 $\mu\text{m}/\text{step}$. Once the exact distance between reference mirror and sample is known, we can always find the same vertical position of the sample. Using this feedback method, we could reduce the uncertainty level down to 0.6 % and 0.3 % below and above 100 cm^{-1} , respectively.

3. Results and Discussions

3.1. Reflectivity and Optical Conductivity

Figure 1 shows the reflectivity spectra, $R(\omega)$, of LiFeAs single crystal at different temperatures. $R(\omega)$ in normal state above T_c (=17.6 K) decreases to follow the Hagen-Rubens relation in the frequency range from 20 to ~ 100 cm^{-1} , which indicates the metallic behavior of LiFeAs. The 4 K data shows a clear signature of the development of the SC state in reflectivity when it approaches unity below 25 cm^{-1} within the uncertainty level of 0.6 %. This behavior in reflectivity is an undeniable evidence of the SC gap formation. The bottom inset of Figure 1 shows the reflectivity spectra for

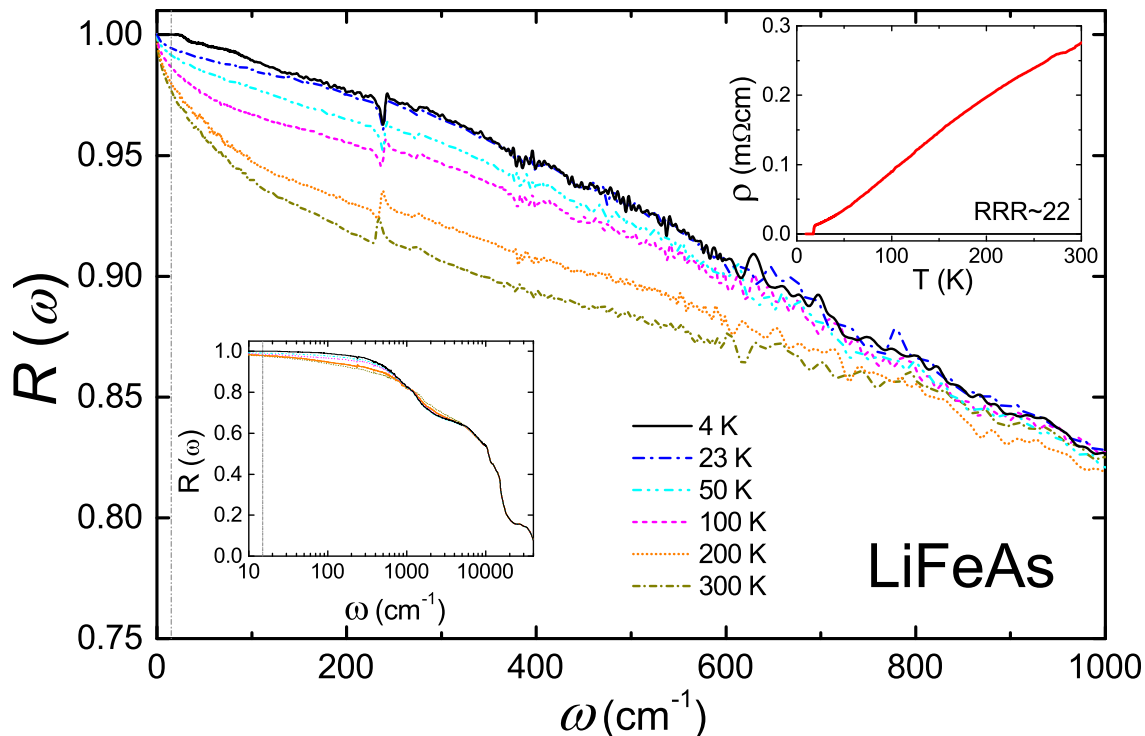


Figure 1. (color online). Reflectivity spectra, $R(\omega)$, of LiFeAs ($T_c = 17.6$ K) in the low frequency region for various temperatures. The normal state data below 15 cm^{-1} (dashed line) were extrapolated using the Hagen-Rubens formula. The bottom inset shows reflectivity in the frequency up to $40,000 \text{ cm}^{-1}$. The top inset shows the electrical resistivity of LiFeAs single crystal and indicates the Residual Resistivity Ratio (RRR) ~ 22 of our sample.

overall range of the measured frequencies. In the infrared region, two knee-like steps were observed at 800 and $2,500 \text{ cm}^{-1}$. These steps in the reflectivity spectra are caused by interband transitions. The top inset of Fig. 1 is the resistivity data, measured by the standard four probe method, showing the SC transition at 17.6 K with $\text{RRR} \sim 22$.

For more convenient analysis, the real part of optical conductivity $\sigma_1(\omega)$ was calculated using the KK transformation from our reflectivity data. Following the standard procedure, Hagen-Rubens formula was used for the low frequency extension below 15 cm^{-1} with the value obtained from electrical resistivity for normal state. Figure 2 shows the results of $\sigma_1(\omega)$ at different temperatures. In normal state, $\sigma_1(\omega)$ decreases from dc value with increasing frequency which is a typical feature of the Drude response. Furthermore, the width of the low frequency Drude part of $\sigma_1(\omega)$ rapidly decreases with decreasing temperature which indicates the systematic evolution of the coherent metallic state with decreasing temperature up to T_c .

In the mid-IR region, two sharp peaks are observed at 240 and 270 cm^{-1} . Jishi *et al.* [36] reported the calculated frequencies of IR-active phonon modes at $228 (E_u)$,

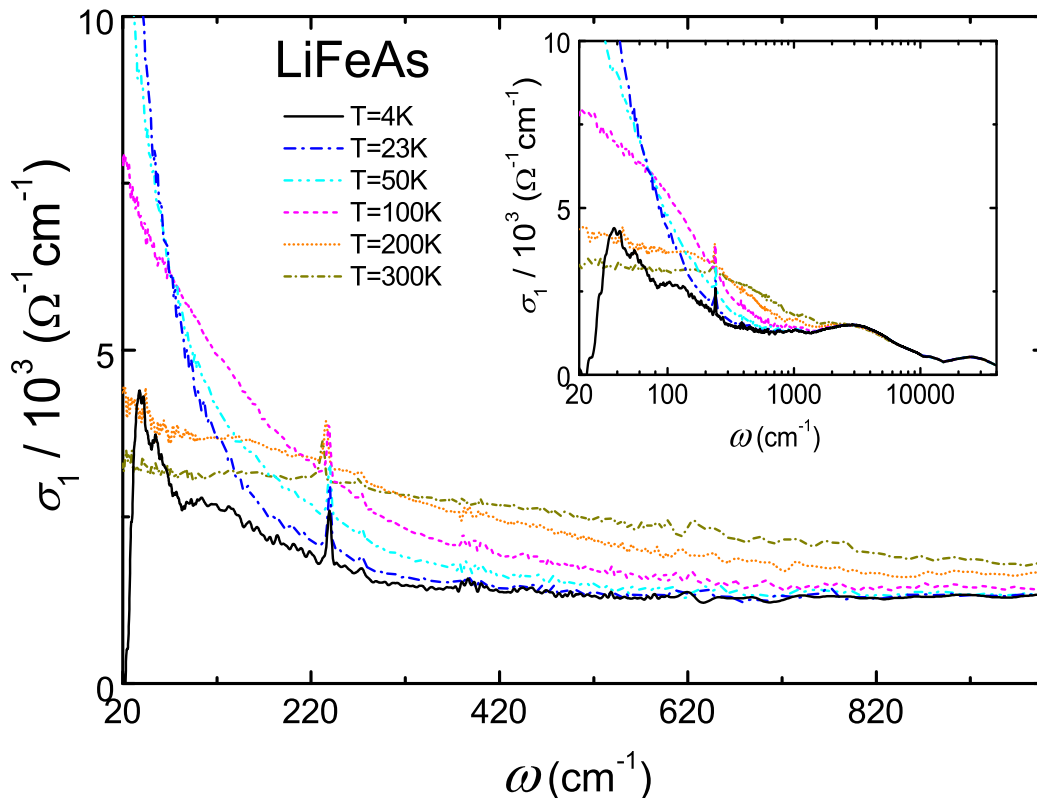


Figure 2. (color online). Real part of the optical conductivity, $\sigma_1(\omega)$, of LiFeAs in the low frequency region for various temperatures. The inset shows $\sigma_1(\omega)$ up to 40,000 cm^{-1} .

276 (E_u), 277 (E_u) and 338 (A_{2u}) cm^{-1} in LiFeAs. By comparison, these two peaks of our experimental data correspond to the IR-active phonons. Interesting behavior of these IR-active phonon peaks is their strong temperature dependence; its peak intensity becomes rapidly sharper as decreasing temperature. Similar behavior was observed in infrared study of BaFe_2As_2 and was explained by orbital ordering in the Fe-As layers [37]. We suspect that a similar orbital ordering might occur in LiFeAs.

Below T_c , the 4 K data shows a dramatic change in the low frequency region: a sudden drop and vanishing of the optical absorptions below 25 cm^{-1} . This change in the optical conductivity below T_c should arise from the formation of SC energy gap. Our 4 K data of $\sigma_1(\omega)$ is practically zero below 25 cm^{-1} , within the uncertainty level of 0.6 %. This complete suppression of the optical absorption is also reflected in the reflectivity data with $R(\omega) \rightarrow 1$ below T_c (see Fig.1). In the clean limit superconductivity, no optical excitations exist at the frequencies lower than twice the SC gap magnitude (2Δ) [38], hence we conclude that our LiFeAs sample is a clean limit superconductor. Assuming the sign-changing multiple s-wave pairing state, as generally accepted for most of the iron based superconductors, this clean limit opening of the optical absorption gap implies that the interband impurity scattering is absent or very weak [39]. On the other hand, the fat Drude spectra at normal state (the full width half maximum of it at 23 K is about

60 cm^{-1}) and the significant absorption spectra above the absorption edge $\omega > 2\Delta$ in the SC state imply that there should exist a sufficient amount of scattering both in normal and SC states. The reconciliation between the clean limit SC behavior and the large scattering rate even below T_c leads us to the following scenario for the scattering: (1) the impurity scattering should be very weak; (2) the strong inelastic scattering exists and its low energy part is cut off when the system enters the SC phase, indicating its dynamic coupling with the free carriers of the Drude component.

3.2. Drude-Lorentz model analysis

In order to understand the further details of the electronic structure of LiFeAs, we have analyzed the normal state $\sigma_1(\omega)$ using the standard Drude-Lorentz model in which the optical absorptions are described by separate contributions of the delocalized carriers at low frequencies and the excitations of the bound electrons at the high frequency region. Thus we fit our data $\sigma_1(\omega)$ using the following formula:

$$\sigma(\omega) = \frac{1}{4\pi} \left[\sum_j \frac{\omega_{P,j}^2}{\frac{1}{\tau_{D,j}} - i\omega} + \sum_k S_k \frac{\omega}{\tau_{L,k} + i(\omega_{0,k}^2 - \omega^2)} \right] \quad (1)$$

where $\omega_{P,j}^2 = 4\pi n_j e^2 / m_j^*$ and $1/\tau_{D,j}$ are the plasma frequency squared, scattering rate for the j -th band, respectively, and S_k , $\omega_{0,k}$ and $1/\tau_{L,k}$ are the strength, center and width of the k -th oscillation, respectively. First, we tried one Drude band fitting for the low frequency Drude part of the 23K data but failed, and we found at least two Drude bands are necessary and the fitting was successful as shown in Fig.3(b). Then the rest of the high frequency spectral density can be optimally fitted with seven Lorentzian oscillators. This result is shown in Fig.3(b) and the fitting parameter values are listed in Table 1.

Then we fit the low frequency Drude part of the 300K data with the same two Drude bands as used in the 23K data. We found that two Drude bands with the same plasma frequencies but only with the increased scattering rates fit the data very well. Also the rest of the high frequency spectra was well fitted with the same seven Lorentzian oscillators with almost same fitting parameters as used in the 23K data. This result is summarized in Table 1. Therefore, the main difference between the 23K data and 300K data is the temperature evolution of the Drude part with decreasing scattering rates with decreasing temperature. On the other hand, the Lorentzian oscillator part shows almost no change with temperature and we believe that their origin is the interband transition as confirmed with the band calculations in the next section. The total plasma frequency estimated by f -sum rule of the two fitted Drude terms is $\omega_p = 8224.4 \text{ cm}^{-1}$, which is about 10 % smaller than that of 122 superconductors reported already [19, 17]. The scattering rates of the Drude spectra are also smaller compared to the other Fe-based superconductors [19, 17]. These facts might be concomitantly related with the moderate $T_c \approx 17\text{K}$ of LiFeAs. To have more comparison, the optimal doped 11 compound, $\text{FeTe}_{0.55}\text{Se}_{0.45}$ [28], which has slightly lower $T_c \sim 14\text{K}$ than our 111 compound, has a slightly smaller value of the total Drude plasma frequency $\omega_p \sim 7200 \text{ cm}^{-1}$.

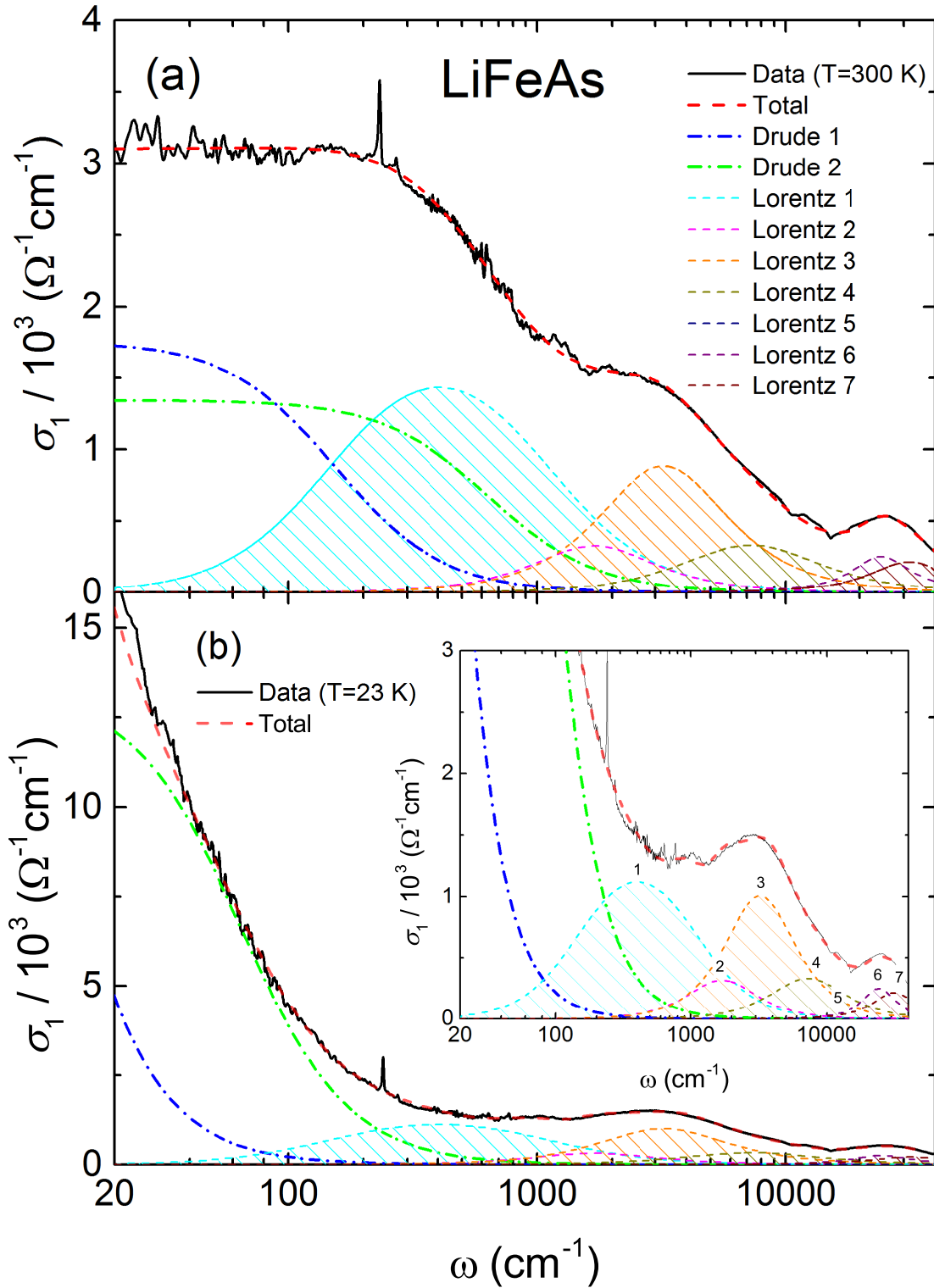


Figure 3. (color online). The results of the best fit for the optical conductivity of the 300 K (a) and 23 K data (b) with two Drude components and seven Lorentzian oscillators. Inset of (b) shows a close up view of the $T = 23 \text{ K}$ data fitting

(A) Drude Spectra Parameters			
T (K)	Drude band	$\omega_{P,j}$ (cm ⁻¹)	$1/\tau_{D,j}$ (cm ⁻¹)
23	Drude 1	4,033	8
	Drude 2	7,173	65
300	Drude 1	4,032	154
	Drude 2	7,173	637

(B) Lorentz Oscillators Parameters			
23K	S_k	$\omega_{0,k}$ (cm ⁻¹)	$1/\tau_{L,k}$ (cm ⁻¹)
Lorentz 1	1.25	403	1210
Lorentz 2	0.75	1694	2500
Lorentz 3	4.64	3226	5001
Lorentz 4	3.71	7259	12099
Lorentz 5	0.03	12099	8066
Lorentz 6	3.85	24359	16535
Lorentz 7	5.60	31456	28230
300K	S_k	$\omega_{0,k}$ (cm ⁻¹)	$1/\tau_{L,k}$ (cm ⁻¹)
Lorentz 1	1.60	403	1210
Lorentz 2	0.75	1694	2500
Lorentz 3	4.08	3226	5001
Lorentz 4	3.71	7259	12099
Lorentz 5	0.03	12099	8066
Lorentz 6	3.85	24359	16535
Lorentz 7	5.60	31456	28230

Table 1. Parameters of the Drude-Lorentz fit of the optical conductivity of the 23 and 300 K data (Data of Fig.3). (a) $\omega_{p,j}$ and $1/\tau_{D,j}$ are the plasma frequency and scattering rate of the j -th Drude band, respectively. (b) S_k , $\omega_{0,k}$, and $1/\tau_{L,k}$ are the oscillator strength, the resonance frequency, and the width of the k -th Lorentzian oscillator, respectively.

We can also extract some more information from our fitting values of Drude spectra. The plasma frequency of Drude-2 band is much larger than that of Drude-1 band, which indicates that the FS of the Drude-2 band is much larger than the FS of the Drude-1 band. Also, the drastic decrease of the scattering rates ($1/\tau_{D,j}$) from 300K to 23K (see Table 1.(A)) indicates that the dominant scattering process must be of inelastic origin and the contribution from the impurity scattering must be very weak. This is also consistent with the fact that the most possible origin of impurities in LiFeAs is the Li vacancies which are located above the conducting Fe-As layers. The analysis using the Drude-Lorentz model with two Drude components was already employed in several optical spectroscopy studies of the iron based superconductors [24, 27, 37]. Indeed, various other experimental and theoretical studies also pointed out the multiband

features and the weak interband scattering in LiFeAs superconductor [40, 41, 42, 43].

3.3. Lorentz oscillators and Interband transitions

In order to have a direct comparison of the theoretical electronic structure of LiFeAs with our optical measurement, we have calculated the direct interband transitions in $\sigma_1(\omega)$ using the band calculation results and have compared them to the Lorentz oscillators of our optical conductivity data. The LDA calculation for the band structures was performed with WIEN2k code and the interband transitions of $\sigma_1(\omega)$ spectra were derived from a standard formula as follows [46];

$$\sigma(\omega) = \frac{\pi e^2}{m_0^2 \omega} \sum_{\mathbf{k}} \sum_{nn'} \frac{|\langle n'\mathbf{k} | \mathbf{e} \cdot \mathbf{p} | n\mathbf{k} \rangle|^2}{\omega - \omega_{nn'}(\mathbf{k}) + i\Gamma} \times \frac{f(\epsilon_{n\mathbf{k}}) - f(\epsilon_{n'\mathbf{k}})}{\omega_{nn'}(\mathbf{k})} \quad (2)$$

Here, the $|n'\mathbf{k}\rangle$ and $|n\mathbf{k}\rangle$ states denote the unoccupied and occupied states, respectively, \mathbf{e} and \mathbf{p} are the polarization of light and the momentum of the electron, respectively, $f(\epsilon_{n\mathbf{k}})$ is the Fermi-Dirac distribution function, $\hbar\omega_{nm} = \epsilon_{n\mathbf{k}} - \epsilon_{m\mathbf{k}}$ is the energy difference between the unoccupied and occupied states, and Γ is the lifetime. In the calculation, $\Gamma = 1$ meV was assumed. The band structure near the Fermi level is shown in Fig. 4 (a) with some of the bands labelled. The experimental result at $T = 23$ K and the calculated spectra of $\sigma_1(\omega)$ are displayed together in Figure 4 (b) and 4 (c). Here, two Drude parts from the fit were subtracted from the experimental data because the calculation with Eq. (2) included only the interband transition processes. The calculated optical spectra have peaks at around 250, 1,300, 3,000, 6,500, 12,000 and 25,000 cm^{-1} , respectively. The origin of each peak is denoted in the legend of Figure 4 (b) as A to G. For example, the peak at 1,300 cm^{-1} (denoted as B) is due to the interband transitions from #61, 62 to #63, 64 labelled bands. The peak positions are in good agreement with experimental result (pointed by dotted lines in Figure 4 (b)) while the peak intensities are not as good in agreement with the experimental data as in the peak position. This is understandable because Eq. (2) is using a very simple coupling matrix $\sim 1/m_0$ and the actual optical coupling matrices should be more complicated. The overall intensity of the calculated $\sigma_1(\omega)$ below 10,000 cm^{-1} is qualitatively consistent with experimental spectra. However, the intensity of the calculated $\sigma_1(\omega)$ above 10,000 cm^{-1} is much larger than the experimental value. Also the spectra above 10,000 cm^{-1} have large overlap of the multitude of the transitions between several bands thus the origin of the peaks becomes harder to identify.

3.4. Optical Conductivity in Superconducting State

As shown in Fig. 2, the change of the optical conductivity from 23 K to 4 K in the low frequency range clearly indicates the formation of a SC energy gap. The SC plasma frequency (ω_{ps}) can be estimated from the spectral weight transfer. According to the Ferrell-Glover-Tinkham (FGT) sum rule [47, 48], the spectral weight difference in the optical conductivity data between just above T_c and much below T_c (so called the missing

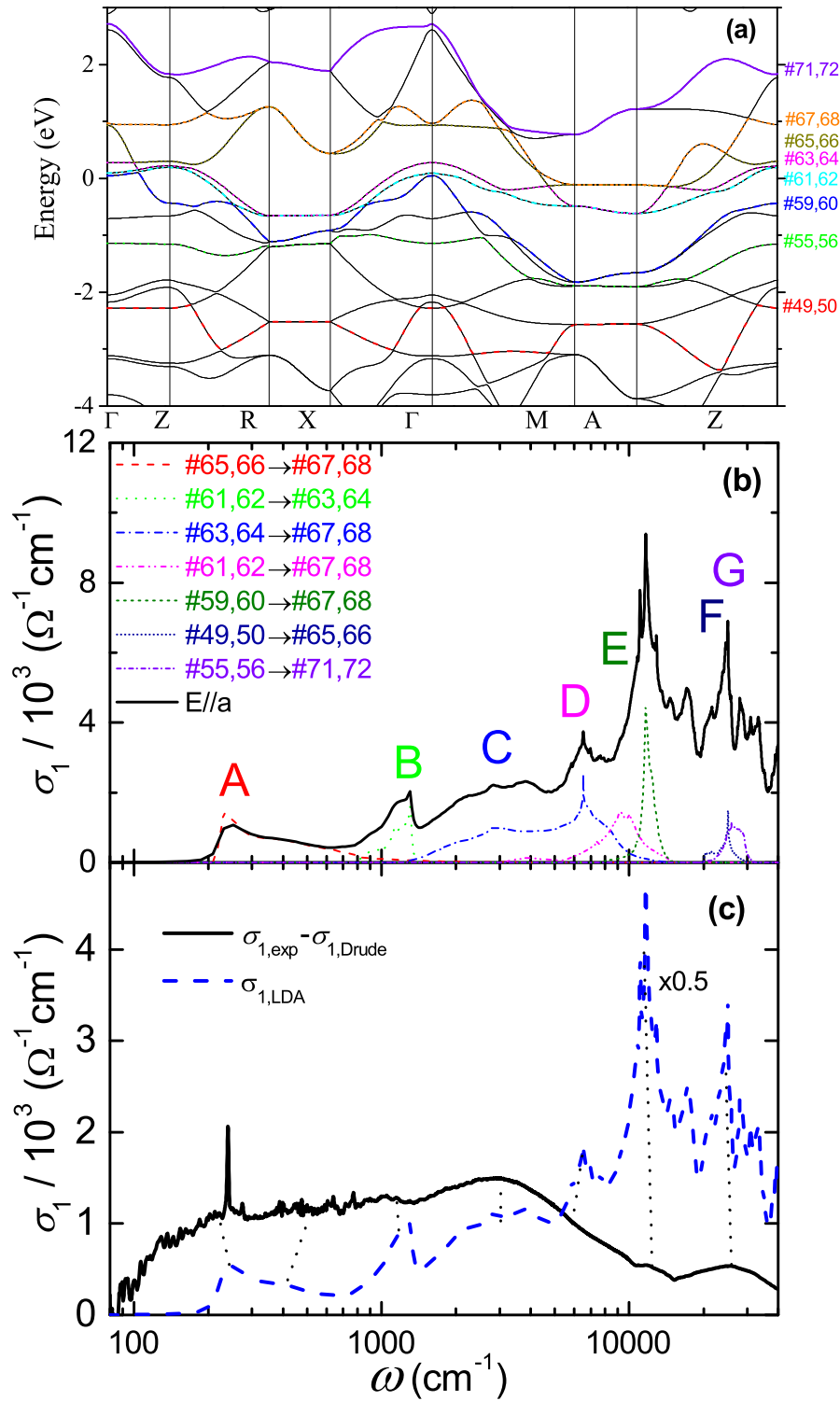


Figure 4. (color online). (a) Calculated band structure of LiFeAs near the Fermi level, (b) Calculated interband transition contributions to $\sigma_1(\omega)$ of LiFeAs. The total (black solid) and the separated band-to-band contributions. (A: #65,66 \rightarrow #67,68, B: #61,62 \rightarrow #63,64, C: #63,64 \rightarrow #67,68, D: #61,62 \rightarrow #67,68, E: #59,60 \rightarrow #67,68, F: #49,50 \rightarrow #65,66 and G: #55,56 \rightarrow #71,72), (c) Comparison between the calculated (blue dashed line) and experimental (black solid line) optical conductivity spectra at $T = 23$ K.

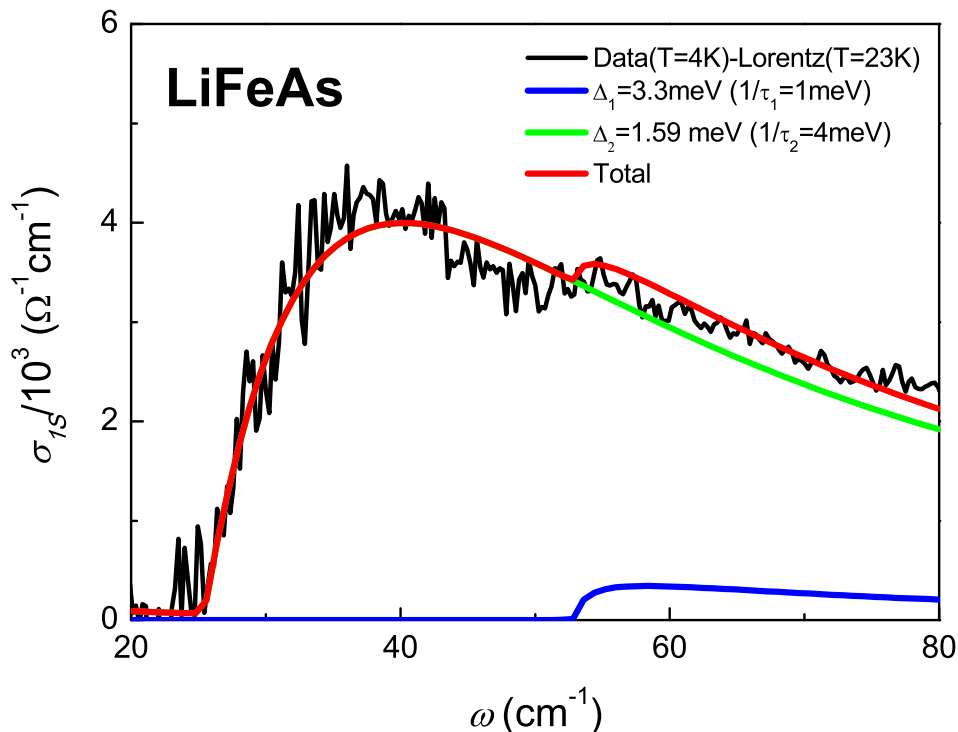


Figure 5. (color online). Fitting of the low frequency optical conductivity (σ_{1S}) of SC state (4 K data) using the generalized Mattis-Bardeen formula [33]. Two bands fitting is required and the estimated SC energy gap values, corresponding to the Drude-1 and Drude-2 bands of the normal state, are $\Delta_1 = 3.3$ meV and $\Delta_2 = 1.59$ meV with the corresponding scattering rates $1/\tau_1 = 1$ meV and $1/\tau_2 = 4$ meV, respectively.

area) indicates the condensation strength and determines the condensation density of the free carriers, which is described as follows [47, 48]:

$$\omega_{ps}^2 = 8 \int_0^{\omega_c} [\sigma_1(\omega, T \cong T_c) - \sigma_1(\omega, T \ll T_c)] d\omega \quad (3)$$

where $\omega_{ps}^2 = 4\pi n_s e^2 / m^*$. The cut-off frequency (ω_c) was set as $1,000 \text{ cm}^{-1}$ because there is almost no difference between 23 K and 4 K data. SC plasma frequency (ω_{ps}) can also be evaluated by the zero crossing of the dielectric function, $\epsilon_1(\omega) \approx \epsilon_\infty - \omega_{ps}^2 / \omega^2$ ($\epsilon_\infty \approx 3.6$), and by the zero frequency limit of the real part of $[-\omega^2 \epsilon_1(\omega)]^{0.5}$. All three methods consistently yield $\omega_{ps} \sim 6,665 \pm 140 \text{ cm}^{-1}$. Combining with the previous estimate of $\omega_p = 8224.4 \text{ cm}^{-1}$, we obtained $(\omega_{ps} / \omega_p)^2 \sim 0.65$, which indicates that more than a half of the free carriers of the normal state condensates. The penetration depth evaluated from the relation $\lambda = c / \omega_{ps}$ is 238 nm, which is about 10% larger than the already reported results [17, 19, 49].

The low frequency optical conductivity (σ_{1S}) of the 4K data is separately displayed in Figure 5. The data clearly shows the opening of the optical absorption gap below approximately 25 cm^{-1} due to the formation of the SC gap. The theoretical calculation

based on the isotropic s-wave gaps using the generalized Mattis-Bardeen formula [33] was used to fit the data. Here we fitted the data of $\sigma_{1S}(\omega)$ with two bands with two independent s-wave gaps, which is consistent with the two Drude components analysis of the normal state $\sigma_{1N}(\omega)$ in the previous section. The results are in excellent agreement with the experimental data as shown in Figure 5. The SC gaps (and scattering rates) were estimated to be $\Delta_1 = 3.3$ meV ($1/\tau_1 = 1$ meV) and $\Delta_2 = 1.59$ meV ($1/\tau_2 = 4$ meV). The gap to T_c ratios are, $2\Delta_{1,2}/k_B T_c \sim 4.5$ and 2.17 , respectively, as compared to the BCS weak coupling limit ($= 3.5$). These values may be consistently compared with other iron-based SC compounds; for example, the optimal doped 11-compound, $\text{FeTe}_{0.55}\text{Se}_{0.45}$ ($T_c \sim 14\text{K}$)[28], has slightly smaller values of the SC gaps, $\Delta_1 = 2.5$ meV and $\Delta_2 = 1.25$ meV, respectively.

We also found that the band with a larger spectral weight (Drude-2 band, $\omega_{P,2} = 7,173$ cm^{-1}) opens a smaller gap $\Delta_2 = 1.59$ meV and the band with a smaller spectral weight (Drude-1 band, $\omega_{P,1} = 4,033$ cm^{-1}) opens a larger gap $\Delta_1 = 3.3$ meV. This inverse proportionality between the SC gap size and the spectral weight of the two Drude bands is consistent with the prediction of the s_{\pm} -wave pairing scenario mediated by the interband repulsive interaction[50]. Our result of the two SC gaps is consistent with the observation of other experiments by specific heat [12], ARPES [43], NMR[44] measurements, and also with a theoretical prediction[45]. Also the scattering rates $1/\tau_{1,2}$ obtained from the Mattis-Bardeen formula are consistently close to the values of $1/\tau_{D,j}$ of the Drude-1 and the Drude-2 bands of the normal state, indicating that the SC gaps are indeed formed in the Drude-1 and the Drude-2 bands, respectively. Some discrepancy is due to the fact that the generalized Mattis-Bardeen formula is not directly derived from the Drude formula.

4. Conclusions

We have measured the optical properties of the iron based superconductor LiFeAs single crystal ($T_c = 17.6$ K) at various temperatures from the tera-hertz to violet frequency regions and have successfully – for the first time with the optical spectroscopy - deduced the multi-band nature of LiFeAs both in the SC and normal states. The optical spectra in the normal state is well described by the Drude-Lorentz model assuming two Drude components with $\omega_{D,1} = 4,033$ cm^{-1} and $\omega_{D,2} = 7,173$ cm^{-1} , respectively. In the SC state at $T = 4$ K, a clean gap opening is observed in our optical conductivity data below T_c and the theoretical fitting using the generalized Mattis-Bardeen model [33] identifies the two isotropic SC gaps of $\Delta_1 = 3.3$ meV and $\Delta_2 = 1.59$ meV, respectively. These results confirm that the multi-band nature is essential to understand the electronic properties of LiFeAs both in the normal state and SC state in accord with various other experiments. Furthermore, we have extracted the inverse proportionality between the SC gap size and the spectral weight of the two Drude bands. This finding is an indirect evidence supporting the pairing scenario mediated by the interband pairing interaction[50].

The total SC plasma frequency was estimated $\omega_{ps} \sim 6,665$ cm^{-1} and it corresponds

to an effective penetration depth of $\lambda = 238$ nm. From the comparison with the total normal state plasma frequency $\omega_p \sim 8,224.4$ cm⁻¹, this implies that about 65 % of the free carriers of the normal state condenses in the SC state and about 35% of the free carriers still remains un-condensed. As seen in Figure 5, the existence of the substantial amount of the un-condensed incoherent spectra above the optical gap as well as the clean gap opening below ~ 25 cm⁻¹ reveal the several important facts: (1) our LiFeAs single crystal is a clean limit superconductor with a very weak impurity scattering; (2) nevertheless, it has a strong inelastic scattering which causes the pair-breaking process above the optical gap; (3) and this inelastic scattering should also develop the excitation gap as a low energy cut-off when the system enters the SC state, meaning that this bosonic inelastic scattering is dynamically coupled to the free carriers. Finally, we identified the several Lorentzian oscillators observed in our optical data over the mid-IR to violet region with the interband optical transitions by using the LDA band structure calculations.

Acknowledgments

This work was supported by the Basic Science Research Program (2010-0007487), the Mid-career Researcher Program (2010-0029136), and the Leading Foreign Research Institute Recruitment Program (Grant No. 2012K1A4A3053565) through the National Research Foundation of Korea (NRF) funded by the Ministry of Education, Science and Technology (MEST). YB was supported by grant numbers NRF-2010-0009523 and NRF-2011-0017079.

References

- [1] Kamihara Y, Watanabe T, Hirano M and Hosono H 2008 *J. Am. Chem. Soc.* **130** 3296
- [2] Ren Z A, Che G C, Dong X L, Yang J, Lu W, Yi W, Shen X L, Li Z C, Sun L L, Zhou F and Zhao Z X 2008 *EPL* **83** 17002
- [3] Chen X H, Wu T, Wu G, Liu R H, Chen H and Fang D F 2008 *Nature* **453** 761
- [4] Rotter M, Tegel M and Johrendt D *Phys. Rev. Lett.* **101** 107006
- [5] Ren Z, Zhu Z, Jiang S, Xu X, Tao Q, Wang C, Feng C, Cao G and Xu Z 2008 *Phys. Rev. B* **78** 052501
- [6] Lee H, Park E, Park T, Sidorov V A, Ronning F, Bauer E D and Thompson J D 2009 *Phys. Rev. B* **80** 024519
- [7] Hsu F C, Luo J Y, Yeh K W, Chen T K, Huang T W, Wu P M, Lee Y C, Huang Y L, Chu Y Y, Yan D C and Wu M K 2009 *Proc Natl Acad Sci USA* 105(38):14262
- [8] Song Y J, Ghim J S, Min B H, Kwon Y S, Jung M H and Rhyee J S 2010 *Appl. Phys. Lett.* **96** 212508
- [9] Tapp J H, Tang Z, Lv B, Sasmal K, Lorenz B, Chu P C W and Guloy A M 2008 *Phys. Rev. B* **78** 060505
- [10] Singh D J 2008 *Phys. Rev. B* **78** 094511
- [11] Nakamura H, Machida M, Koyama T and Hamada N 2009 *J. Phys. Soc. Jpn.* **78** 123712
- [12] Stockert U, Abdel-Hafiez M, Evtushinsky D V, Zabolotnyy V B, Wolter A U B, Wurmehl S, Morozov I, Klingeler R, Borisenko S V, Buchner B, 2011 *Phys. Rev. B* **83** 224512

- [13] Borisenko S V, Zabolotnyy V B, Evtushinsky D V, Kim T K, Morozov I V, Yaresko A N, Kordyuk A A, Behr G, Vasiliev A, Follath R and Büchner B 2010 *Phys. Rev. Lett.* **105** 067002
- [14] Wei F, Chen F, Sasmal K, Lv B, Tang Z J, Xue Y Y, Guloy A M and Chu C W 2010 *Phys. Rev. B* **81** 134527
- [15] Jang D J, Hong J B, Kwon Y S, Park T, Gofryk K, Ronning F, Thompson J D and Bang Y 2012 *Phys. Rev. B* **85** 180505(R)
- [16] Imai Y, Takahashi H, Kitagawa K, Matsubayashi K, Nakai N, Nagai Y, Uwatoko Y, Machida M and Maeda A 2011 *J. Phys. Soc. Jpn.* **80** 013704
- [17] Kim H, Tanatar M A, Song Y J, Kwon Y S and Prozorov R 2011 *Phys. Rev. B* **83** 100502
- [18] Sasmal K, Lv B, Tang Z, Wei F Y, Xue Y Y, Guloy A M and Chu C W 2010 *Phys. Rev. B* **81** 144512
- [19] Song Y J, Ghim J S, Yoon J H, Lee K J, Jung M H, Ji H S, Shim J H, Bang Y and Kwon Y S 2011 *EPL* **94** 57008
- [20] Um Y J, Park J T, Min B H, Song Y J, Kwon Y S, Keimer B and Tacon M L 2012 *Phys. Rev. B* **85** 012501
- [21] Qazilbash M M, Hamlin J J, Baumbach R E, Zhang L, Singh D J, Maple M B and Basov D N 2009 *Nature Phys.* **5** 647
- [22] Dong J, Zhang H J, Xu G, Li Z, Li G, Hu W Z, Wu D, Chen G F, Dai X, Luo J L, Fang Z and Wang N L 2008 *EPL* **83** 27006
- [23] Barišić N, Wu D, Dressel M, Li L J, Cao G H and Xu Z A 2010 *Phys. Rev. B* **82** 054518
- [24] Kim K W, Rössle M, Dubroka A, Malik V K, Wolf T and Bernhard C 2010 *Phys. Rev. B* **81** 214508
- [25] Wu D, Barišić N, Dressel M, Cao G H, Xu Z, Schachinger E and Carbotte J P 2010 *Phys. Rev. B* **82** 144519
- [26] Li G, Hu W Z, Dong J, Li Z, Zheng P, Chen G F, Luo J L and Wang N L 2008 *Phys. Rev. Lett.* **101** 107004
- [27] Tu J J, Li J, Liu W, Punnoose A, Gong Y, Ren Y H, Li L J, Cao G H, Xu A A and Homes C C 2010 *Phys. Rev. B* **82** 174509
- [28] Homes C C, Akrap A, Wen J S, Xu Z J, Lin Z W, Li Q and Gu G D 2010 *Phys. Rev. B* **81** 180508(R)
- [29] Maksimov E G, Karakozov A E, Gorshunov B P, Prokhorov A S, Voronkov A A, Zhukova E S, Nozdrin V S, Zhukov S S, Wu D, Dressel M, Haindl S, Iida K and Holzapfel B 2011 *Phys. Rev. B* **83** 140502(R)
- [30] Charnukha A, Deisenhofer J, Propper D, Schmidt M, Wang Z, Goncharov Y, Yaresko A N, Tsurkan V, Keimer B, Loidl A and Boris A V 2012 *Phys. Rev. B* **85** 100504(R)
- [31] Chen Z G, Yuan H, Dong T, Xu G, Shi Y G, Zheng P, Luo J L, Guo J G, Chen X L, and Wang N L 2011 *Phys. Rev. B* **83** 220507(R)
- [32] Kwon Y S, Hong J B, Jang Y R, Oh H J, Song Y Y, Min B H, Iizuka T, Kimura S, Balatsky A V, Bang Y 2012 *New J. Phys.* **14** 063009
- [33] Zimmermann W, Brandt E H, Bauer M, Seider E, Genzel L 1991 *Physica C* **183** 99
- [34] Inosov D S, White J S, Evtushinsky D V, Morozov I V, Cameron A, Stockert U, Zabolotnyy V B, Kim T K, Kordyuk A A, Borisenko S V, Forgan E M, Klingeler R, Park J T, Wurmehl S, Vasiliev A N, Behr G, Dewhurst C D and Hinkov V 2010 *Phys. Rev. Lett.* **104** 187001
- [35] Kimura S 2008 *JASCO Rep.* **50** 6 (in Japanese)
- [36] Jishi R A and Alyahyaei H M 2009 *Adv. Cond. Mat. Phys.* **2010** 804343
- [37] Akrap A, Tu J J, Li L J, Cao G H, Xu A A and Homes C C 2009 *Phys. Rev. B* **80** 180502(R)
- [38] Tinkham M 1996 *"Introduction to superconductivity"* (Singapore: McGraw-Hill) p 88
- [39] Bang Y, Choi H Y, Won H 2009 *Phys. Rev. B* **79** 054529
- [40] Hajiri T, Ito T, Niwa R, Matsunami M, Min B H, Kwon Y S and Kimura S 2012 *Phys. Rev. B* **85** 094509
- [41] Ferber J, Foyevtsova K, Valentí R and Jeschke H O 2012 *Phys. Rev. B* **85** 094505

- [42] Hashimoto K, Kasahara S, Katsumata R, Mizukami Y, Yamashita M, Ikeda H, Terashima T, Carrington A, Matsuda Y and Shibauchi T 2012 *Phys. Rev. Lett.* **108** 047003
- [43] Umezawa K, Li Y, Miao H, Nakayama K, Liu Z H, Richard P, Sato T, He J B, Wang D M, Chen G F, Ding H, Takahashi T and Wang S C 2012 *Phys. Rev. Lett.* **108** 037002
- [44] Li Z, Ooe Y, Wang X, Liu Q, Jin C, Ichioka M and Zheng G 2010 *J. Phys. Soc. Jpn.* **79** 083702
- [45] Platt C, Thomale R and Hanke W 2011 *Phys. Rev. B* **84** 235121
- [46] Antonov V, Harmon B and Yaresko A 2004 *Electronic Structure and Magneto-Optical Properties of Solids* (Dordrecht: Kluwer Academic)
- [47] Ferrell R A and Glover III R E 1958 *Phys. Rev.* **109** 1398
- [48] Tinkham M and Ferrell R A 1959 *Phys. Rev. Lett.* **2** 331
- [49] Pratt F L, Baker P J, Blundell S J, Lancaster T, Lewtas H J, Adamson P, Pitcher M J, Parker D R and Clarke S J 2009 *Phys. Rev. B* **79** 052508
- [50] Bang Y, Chio H Y 2010 *Phys. Rev. B* **78** 134523